

1 **Reducing uncertainties in climate projections with emergent**
2 **constraints: Concepts, Examples and Prospects**

3 **Florent Brient¹**

4 ¹CNRM, Université de Toulouse, Météo-France, CNRS, Toulouse France

Corresponding author: Florent Brient, florent.brient@gmail.com

5 Abstract

6 Models disagree on a significant number of responses to climate change, such as climate
7 feedback, regional changes, or the strength of equilibrium climate sensitivity. Emergent con-
8 straints aim to reduce these uncertainties by finding links between the inter-model spread in
9 a observable predictor and climate projections. In this paper, I recall the concepts underlying
10 this framework with an emphasis on the statistical inference used for narrowing uncertain-
11 ties, and review emergent constraints found in the last two decades. I investigate potential
12 links between highlighted predictors, especially those targeting uncertainty reductions in
13 climate sensitivity, cloud feedback, and changes of the hydrological cycle. I also show that
14 the disagreement across emergent constraints do not robustly narrow the spread in climate
15 sensitivity. This calls for weighting the realism of emergent constraints by quantifying the
16 level of physical understanding explaining the relationship. This would also permit more
17 efficient model evaluation and better targeted model development. In the context of the up-
18 coming CMIP6 model intercomparison, I expect a growing number of new predictors and
19 uncertainty reductions which call for robust statistical inferences that allow cross-validation
20 of more likely estimates.

21 1 Introduction

22 For more than two centuries, steadily increasing carbon dioxide concentrations in the
23 atmosphere have been warming the Earth. Today it is 0.8°C warmer than in the preindus-
24 trial period in the middle of the 19th century [Morice *et al.*, 2012]. Global climate models
25 (GCMs) project how this global warming will continue given the expected continuous in-
26 crease in human-made carbon dioxide emissions. While models agree on the sign of a num-
27 ber of climate change signals, they often disagree on their amplitude [Flato *et al.*, 2013]. A
28 well-known example is the equilibrium climate sensitivity (ECS), i.e. the equilibrium global-
29 mean surface temperature increase resulting from a sustained doubling of carbon dioxide
30 concentrations [Gregory *et al.*, 2004]. For decades, models have exhibited widely differing
31 climate sensitivities, yet with a range remaining roughly between 2 and 5°C [Charney *et al.*,
32 1979; Bony *et al.*, 2013]. To correctly predict how much the Earth will warm, one must know
33 at least (1) how carbon dioxide concentration will evolve [Stocker *et al.*, 2013], and (2) the
34 correct value of climate sensitivity.

35 A doubling of the carbon dioxide concentration would warm the Earth by $1.2 \pm 0.1^{\circ}\text{C}$
36 [Dufresne and Bony, 2008]. However, this warming induces changes that can amplify or

37 dampen the initial temperature response through feedback processes [Bony *et al.*, 2006].
38 For example, the CO₂-induced global warming allows the atmosphere to hold more water
39 vapor. This acts as a positive feedback on the surface warming, because water vapor itself
40 is a powerful greenhouse gas that, like CO₂, absorbs and re-emits long-wave radiation back
41 to the surface. This is somewhat compensated by the negative temperature lapse rate feed-
42 back that allows more outgoing long wave emission to be emitted out of the atmosphere. The
43 initial warming also reduces the surface albedo by melting snow and sea-ice, which also con-
44 stitutes a positive feedback because snow and ice are effective reflectors of sunlight. Models
45 agree on the sign and approximately the amplitude of these two feedback processes [Ceppi
46 *et al.*, 2017]. The water vapor, lapse-rate, and ice-albedo feedbacks in isolation enhance the
47 global warming due to increasing CO₂ concentrations to around +2.2°C [Dufresne and Bony,
48 2008]. Models disagree on the cloud response to surface warming, which is primarily why
49 they produce a wide range of ECS values, e.g. between 2.1 and 4.7°C for the CMIP5 model
50 intercomparison [Flato *et al.*, 2013]. Since clouds have dynamical scales in the order of tens
51 to hundreds of meters, climate models with grid boxes of hundred of kilometers cannot ex-
52 plicitly resolve cloud processes. Empirically-based assumptions are thus used to relate unre-
53 solvable small-scale dynamics to properties (temperature, humidity etc.) on the models' grid
54 scale. Those parameterizations are the heart of biases in reproducing the present-day climate
55 and of uncertainties in climate change projections [e.g. Brient *et al.*, 2016]. This calls for
56 new efficient process-oriented methods for understanding leading causes behind these uncer-
57 tainties and for establishing better model evaluation and development.

58 **2 Emergent constraints**

59 **2.1 Definition**

60 Recently, a methodology called emergent constraint has been developed for reducing
61 uncertainties in climate-change projections. This framework is based on :

- 62 1. identifying responses to climate change perturbation in which model disagree (e.g.,
63 cloud feedback)
- 64 2. relating the inter-model spread in the climate-change responses to present-day biases
65 or short-term variations that can be observed.

66 This could be achieved by identifying an empirical relationship between the inter-model
67 spread of an observable variable (hereafter named A) and the inter-model responses B to a

68 given perturbation. The variable A is called the predictor and the variable B the predictand.
69 Because observed measurements of the predictor A can then be used to constrain the mod-
70 els' responses B, the relationship between A and B is called an emergent constraint [*Klein*
71 *and Hall, 2015*]. The variable A may represent a metric that characterize the climate system
72 (humidity, winds,...) or may characterize natural variability (e.g., in the seasonal cycle, or
73 from year to year). The response B can be the global-mean response of the climate system
74 (e.g. ECS) or a local response to perturbations (e.g. a regional climate feedback). Therefore,
75 the goal is to find a predictor that, given its relation to a climate response, emerges as a con-
76 straint on future projections.

77 Once the variable A is estimated observationally, the emergent constraint can be used
78 to assess models' realism and to eventually narrow the spread of climate change projections.
79 As an idealized example, Figure 1 shows a randomly-generated relationship between a pre-
80 dictor A simulated by 29 climate models and a projection of future climate changes (in prin-
81 ciple any climate-change response may be considered). The green distribution represents
82 an observational measurement and its uncertainties. We see that differences in A are signif-
83 icantly associated with differences in B, here with a correlation coefficient of $r=0.83$. By
84 constraining A through observations (green distribution), this example suggests that some
85 models are more realistic and, by inference, are associated with more realistic future climate
86 sensitivities. The degree to which the models' A deviates from the observed A can be used to
87 derive weights for the models to compute a weighted average of the models' response B (see
88 section 2.2.3).

89 **2.2 Criterion and uncertainties**

90 **2.2.1 Physical understanding**

91 An emergent constraint can be trusted if it meets certain criteria. The most important
92 one is an understanding of physical mechanisms underlying the empirical relationship, which
93 is the key to increase the plausibility of a proposed emergent constraint. Several methods
94 have been recently suggested to verify the level of confidence of emergent constraints [*Cald-*
95 *well et al., 2018; Hall et al., 2019*]. One of them consists in checking the reliability of an
96 emergent constraint by developing sensitivity tests that would modify A for some models
97 (if there is a straightforward way of manipulating A). For accurate model comparison, this
98 would require coupled model simulations with global-mean radiative balance as performed

99 for CMIP intercomparison. If the models' behavior after the modification deviates from that
100 expected from the emergent constraint, the relationship may have been found by chance. A
101 study showed that this risk is not negligible [Caldwell *et al.*, 2014], primarily because cli-
102 mate models are not independent but many are derived from each other [Masson and Knutti,
103 2011; Knutti *et al.*, 2013]. Keeping only models with enough structural differences often re-
104 duces the reliability of identified emergent constraints. The search for correlations with no
105 obvious physical understanding could lead to such spurious results. Conversely, if those sen-
106 sitivity tests confirm the inter-model relationship, the credibility of assumed physical mech-
107 anisms and observational constraints on climate change projections increases. Those tests
108 could be performed through a multiparameter multiphysics ensemble that would help (1) dis-
109 entangle structural and parametric influence on the multi-model spread in predictor A and (2)
110 highlight underlying processes explaining the empirical relationship [Kamae *et al.*, 2016].

111 **2.2.2 Observation uncertainties**

112 The second criterion is related to the correct use of observations. Uncertainties tied
113 to the observation of the predictor must be small enough so that not all models remain con-
114 sistent with the data. This criterion may not be satisfied if observations are available only
115 over a short time period (as is the case for the vertical structure of clouds, [e.g. Winker *et al.*,
116 2010]), or if the predictor is defined through low-frequency variability (trends, decadal vari-
117 ability), or if there is a lack of consistency among available datasets (as in the case for global-
118 mean precipitation and surface fluxes, [e.g. Găinușă-Bogdan *et al.*, 2015]). Finally, some *ob-*
119 *servational* constraints rely on parameterizations used in climate models, e.g. reanalysis that
120 use sub-grid assumptions for representing clouds [e.g. Dee *et al.*, 2011] or data product for
121 clouds that use sub-grid assumptions for radiative transfer calculations [Rossow and Schiffer,
122 1999].

123 **2.2.3 Statistical inference**

124 Emergent constraints can allow us to narrow uncertainties and quantify more likely
125 estimates of climate projections, i.e. constrained posterior range of a prior distribution. How-
126 ever, not all emergent constraints should be given the same trust. Hall *et al.* [2019] suggested
127 to relate this trust to the level of physical understanding associated with the emergent rela-
128 tionship. This means making predictions only for confirmed emergent constraints.

129 Posterior estimates are influenced by the way the statistical inference has been per-
130 formed. However, no consensus has yet emerged for this inference. A first method for quan-
131 tifying this constraint is to directly use uncertainties underlying the observational predictor
132 and project it onto the vertical axis using the emergent constraint relationship. This method
133 takes into account uncertainties in both observations and the estimated regression model,
134 through bootstrapping samples for instance [Huber *et al.*, 2011]. Most studies use this straight-
135 forward framework. In our idealized example, this would give a posterior estimate of 4.0 ± 0.5
136 (narrower than the raw estimate as seen on Figure 1). However, several problems with this
137 kind of inference might be highlighted:

- 138 • Most fundamentally, the inference generally revolves around assuming that there ex-
139 ists a linear relationship, and estimating parameters in the linear relationship from
140 climate models. But it is not clear that such a linear relationship does in fact exist,
141 and estimating parameters in it is strongly influenced by models that are inconsistent
142 with the observations (extreme values). In other words, the analysis neglects struc-
143 tural uncertainty about the adequacy of the assumed linear model, and the parameter
144 uncertainty the analysis does take into account is strongly reduced by models that are
145 "bad" by this model-data mismatch metric. Outliers thus strongly influence the result.
146 However, the influence of models consistent with the data but off the regression line is
147 diminished. Given that there is no strong a priori knowledge about any linear relation-
148 ship – this is why it is an "emergent" constraint – it seems inadvisable to make one's
149 statistical inference strongly dependent on models that are not consistent with the data
150 at hand.
- 151 • Often analysis parameters are chosen so as to give strong correlations between the re-
152 sponse of models to perturbations and the predictor. This introduces selection bias in
153 the estimation of the regression lines. This leads to underestimation of uncertainties
154 in parameters, such as the slope of the regression line, which propagates into underes-
155 timated uncertainties in the inferred estimate.
- 156 • When regression parameters are estimated by least squares, the observable on the hor-
157 izontal axis is treated as being a known predictor, rather than as being affected by er-
158 ror (e.g., from sampling variability). This likewise leads to underestimation of uncer-
159 tainties in regression parameters. This problem can be mitigated by using errors-in-
160 variables methods.

161 A second method consists of estimating a posterior distribution by weighting each
162 model's response by the likelihood of the model given the observations of the predictor.
163 This can be accomplished by a Bayesian weighting method [e.g. *Hargreaves et al.*, 2012]
164 or through information theory [e.g. *Brient and Schneider*, 2016], such as the Kullback-Leibler
165 divergence or relative entropy [*Burnham and Anderson*, 2010]. This method does not use the
166 linear regression for estimating the posterior distribution and therefore favor realistic models
167 and deemphasize outliers inconsistent with observations. The Kullback-Leibler divergence
168 applied to our idealized example (assuming an identical standard deviation between observa-
169 tion and each model) suggests an estimate of 3.4 ± 0.7 (Figure 1).

170 This more justifiable inference still suffers from several shortcomings. For example,
171 it suffers from selection bias, and it treats the model ensemble as a random sample (which it
172 is not). It also only weights models, suggesting that climate projections far outside the range
173 of what current models produce will always come out as being very unlikely. Given uncer-
174 tainties underlying each method, posterior estimates should thus be quantified using different
175 methods (as previously done in *Hargreaves et al.* [2012] for instance) and methods should be
176 significantly described.

177 Figure 2 provides a tangible example for explaining the importance of statistical infer-
178 ence. It shows the relation in 29 current climate models between ECS and the strength with
179 which the reflection of sunlight in tropical low-cloud regions covaries with surface tempera-
180 ture [*Brient and Schneider*, 2016]. That is, the horizontal axis shows the percentage change
181 in the reflection of sunlight per degree surface warming, for deseasonalized natural varia-
182 tions. It is clear that there is a strong correlation (correlation coefficient about -0.7) between
183 ECS on the vertical axis and the natural fluctuations on the horizontal axis (an example of
184 an empirical fluctuation-dissipation relation in the models). The green line on the horizon-
185 tal axis indicates the probability density function (PDF) of the observed natural fluctuations.
186 What many previous emergent-constraint studies have done is to take such a band of obser-
187 vations and project it onto the vertical ECS axis using the estimated regression line between
188 ECS and the natural fluctuations, taking into account uncertainties in the estimated regres-
189 sion model. If we do this with the data here, we obtain an ECS that likely lies within the blue
190 band: between 3.1 and 4.2 K, with a most likely value of 3.6 K. Simply looking at the scatter
191 of the 29 models in this plot indicates that this uncertainty band is too narrow. For example,
192 model 7 is consistent with the observations, but has a much lower ECS of 2.6 K. The regres-
193 sion analysis would imply that the probability of an ECS this low or lower is less than 4%.

194 Yet this is one of 29 models, and one of relatively few (around 9) that are likely consistent
195 with the data. Obviously, the probability of an ECS this low is much larger than what the re-
196 gression analysis implies. As explained before, these flaws could be reduced by weighting
197 ECS by the likelihood of the model given the observations. Models such as numbers 2 and
198 3, which are inconsistent with observations, would receive essentially zero weight (unlike in
199 the regression-based analysis, they do not influence the final result). No linear relationship is
200 assumed or implied, so models such as 7 receive a large weight because they are consistent
201 with the data, although they lie far from any regression line. The resulting posterior PDF for
202 ECS is shown by the orange line in Figure 1b. The most likely ECS value according to this
203 analysis is 4.0 K. It is shifted upward relative to the regression estimate, toward the values in
204 the cluster of models (around numbers 25 and 26) with relatively high ECS that are consis-
205 tent with the observations. The likely ECS range stretches from 2.9 to 4.5 K. This is perhaps
206 a disappointingly wide range. It is 50 % wider than what the analysis based on linear regres-
207 sions suggests, and it is not much narrower than what simple-minded equal weighting of raw
208 climate models gives (gray line in Figure 1b). But it is a much more statistically defensible
209 range.

210 In order to generalize the sensitivity of inferred estimates to the statistical methodol-
211 ogy, I generate 10^4 random emergent relationships and plot statistics of inferences (mode,
212 confidence intervals) as a function of averaged correlation coefficients. Figure 3 shows that
213 averaged modes and confidence intervals are consistent between the two inference methods
214 for this set of relationships. However, the variance of inferred best estimates (modes) using
215 the weighting method is larger than the one using the inference method. This is in agreement
216 with results obtained from the tangible example from *Brient and Schneider* [2016], which
217 show different most likely values. Therefore, this suggests the best estimate is significantly
218 influenced by the way statistical inference is performed.

219 Finally, uncertainties underlying these estimates may be influenced by the level of
220 structural similarity between climate models. Indeed, adding models with only weak struc-
221 tural differences (e.g. model version with different resolution, interactive chemistry) can ar-
222 tificially strengthen the correlation coefficient of the empirical relationship and the inferred
223 best estimate [*Sanderson et al.*, 2015]. This coefficient is usually the first criterion that quan-
224 tify the statistical credibility of an emergent constraint, i.e. the larger the correlation coeffi-
225 cient, the more trustworthy the regression-based inference will be. However, it remains un-

226 known what level of statistical significance justifies an emergent constraint and whether these
227 correlation best characterize their credibility.

228 **3 Pioneering studies**

229 In the following sections, I aim to describe emergent constraints that have been high-
230 lighted within the last two decades. Table 1 summarize them, along with prior and posterior
231 estimates of the models' predictand. Mean and uncertainties (one standard deviation) are
232 based on the inference provided in the reference if available, or roughly derived through their
233 empirical relationship and observational uncertainties otherwise (for qualitative assessment).

234 In the late 1990s, signs of climate feedback started to be constrained from climate
235 models and observations [e.g. *Hall and Manabe*, 1999]. Usually analyzing one unique model,
236 these studies improved our understanding of physical mechanisms driving climate feedback.
237 However, the lack of inter-model comparisons in these studies did not allow quantifying
238 the relative importance of feedbacks in driving uncertainties in climate change projections.
239 Model intercomparisons during this period identified the cloud response to global warming
240 as being the key contributor of inter-model spread in climate projections [*Cess et al.*, 1990,
241 1996]. Both types of studies thus pave the way toward process-oriented investigation for un-
242 derstanding inter-model differences in climate projections.

243 To my knowledge, the first attempt at introducing the concept of emergent constraint
244 was made by *Allen and Ingram* [2002]. The authors tried to constrain the spread in global-
245 mean future precipitation change simulated by the set of climate models participating in the
246 CMIP2 model intercomparison project [*Meehl et al.*, 2000] through observable temperature
247 variability and a simple energetic framework. Despite the inability to robustly narrow future
248 precipitation changes, they introduced the concepts that establish emergent constraints: the
249 need for physical understanding and the ability of observations to constrain the model predic-
250 tor.

251 An early application of emergent constraints concerns the snow-albedo feedback. *Hall*
252 *and Qu* [2006] showed that differences among models in seasonal northern hemisphere sur-
253 face albedo changes are well correlated with global-warming albedo changes in CMIP3
254 models. The three main criteria for a robust emergent constraint are satisfied: the physical
255 mechanisms are well understood, the statistical relationship between the quantities of inter-
256 est is strong, and uncertainties in the observed variations are weak, allowing the authors to

257 constrain the northern hemisphere snow-albedo feedback under global warming. Despite
258 this successful application, the generation of models that followed (CMIP5) continued to ex-
259 hibit a large spread in seasonal variability of snow-albedo changes [Qu and Hall, 2014]. This
260 could be narrowed through targeted process-oriented model development based on the eval-
261 uation of snow and vegetation parameterizations [Thackeray et al., 2018]. Yet this study can
262 be seen as the first confirmed emergent constraint [Klein and Hall, 2015; Hall et al., 2019].

263 The success of the Hall and Qu study led a number of studies to seek emergent con-
264 straints able to narrow climate-change responses. In the following sections, I review these
265 studies which aim to constrain equilibrium climate sensitivity, cloud feedback, or various
266 changes in Earth system components, such as the hydrological cycle or the carbon cycle.

267 **4 Model biases and equilibrium climate sensitivity**

268 Uncertainties in ECS usually scale with uncertainties in regional climate changes [Senevi-
269 ratne et al., 2016]. So constraining ECS would help estimating regional responses to climate
270 change, which matter the most for impact studies and risk assessment. Therefore, a majority
271 of emergent constraints prioritize providing a better range for ECS, as shown on table 1.

272 The main predictors used to constrain the spread in ECS consist of observable climato-
273 logical characteristics of the current climate. The first study using this approach was Volodin
274 [2008], which found that CMIP3 models with large ECS are more likely to exhibit (1) large
275 differences in cloud cover between the tropics and the extra-tropics and (2) low tropical rela-
276 tive humidity.

277 The first estimate suggested by Volodin [2008] uses a cloud climatology from geo-
278 stationnary satellites to derive a more likely ECS range of 3.6 ± 0.3 K. This range is slightly
279 higher than the multi-model average, with a reduced variance (Table 1). However this study
280 does not address the physical understanding of links between clouds, moisture, and climate
281 feedbacks, which reduce the credibility of this estimate. A more recent study, Siler et al.
282 [2018], provides a physical interpretation underlying this cloud constraint. They hypothe-
283 size that the need for a global-mean radiative balance (through model tuning) forces a link
284 between warm and cold regions, i.e. models having less clouds in the tropical area will very
285 likely simulate more extratropical clouds in the current climate. Given that the global warm-
286 ing will expand tropical warm regions at the expense of extratropical cold regions, these
287 models will increase the spatial coverage of areas with weak cloudiness relative to the multi-

288 model mean, leading to more positive low-cloud feedback and high climate sensitivity. Using
289 observations for characterizing the spatial coverage of cloud albedo, *Siler et al.* [2018] find a
290 best ECS estimate of 3.7 ± 1.3 K, in agreement with *Volodin* [2008].

291 The second estimate suggested by *Volodin* [2008] is related to relative humidity and
292 uses re-analysis outputs to provide a more likely ECS range of 3.4 ± 0.3 K. In CMIP3, mod-
293 els with largest zonal-mean relative humidity over the subtropical free troposphere are those
294 with the lowest climate sensitivity. Given that models generally overestimate this predictor,
295 this suggests the highest ECS values are more realistic. This is in agreement with *Fasullo*
296 *and Trenberth* [2012], which found the same relationship and a best ECS estimate of around
297 4 K (Table 1). This emergent relationship is somewhat explained by the broadening of the
298 tropical dry zones with global warming, which imply a drying of the subsiding branches.
299 Thus, the drier the free troposphere in the current climate the stronger the boundary-layer
300 drying and cloud feedback with global warming. This mechanism may also explain the pos-
301 itive low-cloud feedback in climate models, e.g. the IPSL-CM5A model [*Brient and Bony*,
302 2013]. Conversely, *Volodin* [2008] hypothesized that the relationship is related to the role
303 of relative humidity in convective parameterization. These different physical interpretations
304 suggest that emergent constraints arise from inter-model differences in structural (local) un-
305 certainties, (remote) biases in large-scale dynamics, and the interactions between them.

306 This dichotomy is addressed by *Sherwood et al.* [2014]. They quantify the low-tropospheric
307 convective mixing through the sum of two metrics : an index related to small-scale mixing
308 and an index linked to large-scale mixing. The former aims to represent errors in parameter-
309 ized processes such as shallow convection, turbulence, or precipitation. The latter quantifies
310 model errors in reproducing the tropical dynamical circulation, which can also be affected
311 by parameterizations of deeper convection remotely affecting low-clouds. The CMIP3 and
312 CMIP5 inter-model spread of this predictor is well correlated to uncertainties in ECS. Ob-
313 servations (here reanalysis) suggest that most models underestimate this large-scale mixing,
314 indicating a most likely ECS value larger than 3 K (Table 1). The level of confidence in this
315 estimate is related to the trust one gives to the link between the low-tropospheric character-
316 istics these indices aim to quantify and the low-cloud feedback, which primarily controls the
317 intermodel spread in ECS. The observational constraint should also be viewed with caution
318 since it is based on re-analysis data and hence is influenced by parameterizations.

319 The mixing index suggested by *Sherwood et al.* [2014] highlights that errors in repre-
320 senting the coupling between low-clouds and tropical dynamics explain a significant part of
321 the spread in ECS, in agreement with *Volodin* [2008] and *Fasullo and Trenberth* [2012]. This
322 was confirmed by follow-up studies that suggested significant correlations between ECS and
323 indexes of the tropical dynamics, such as the strength of the double-ITCZ bias [*Tian*, 2015]
324 or the strength of the Hadley circulation [*Su et al.*, 2014]. Both show that models better rep-
325 resenting the tropical large-scale dynamics are those with the highest climate sensitivities
326 (≈ 4 K). However the lack of robust physical mechanisms explaining these emergent con-
327 straints reduces the trustfulness of these inferences, but it also prompts for better theoretical
328 understanding of links between cloud and circulation. This question can be investigated by
329 analyzing the driving influence of clouds on the energetic balance of the atmosphere for ex-
330 plaining large-scale dynamical biases, whether clouds are located in the southern hemisphere
331 [*Hwang and Frierson*, 2013] or in the tropical subsiding regions [*Adam et al.*, 2016, 2017].
332 Together these studies suggest hidden relationships between low clouds, circulation, and cli-
333 mate sensitivity, which remain to be clarified.

334 The spread in ECS can also be constrained through the past variability in global-mean
335 temperature, as suggested by *Cox et al.* [2018]. Observations suggests that a majority of
336 models overestimate temperature variations and year-to-year autocorrelation, providing a
337 most likely posterior ECS estimate of 2.8 ± 0.6 K (Table 1). Contrary to most of emergent
338 constraints, this study thus suggests a relative low best estimate for climate sensitivity. The
339 absence of links between the mathematical framework used to build the predictor and clouds
340 might reduce the confidence in this estimate. However, low-frequency natural variability of
341 tropical temperature seems partly related to cloud variability [e.g *Zhou et al.*, 2016], so it can
342 not be excluded that all these emergent constraints are related to each other. Process-oriented
343 cross-metric analysis would be necessary to support this hypothesis [e.g. *Wagman and Jack-*
344 *son*, 2018].

345 **5 Cloud feedback**

346 The spread of climate sensitivity is significantly related to the spread in cloud feed-
347 back, and mostly to uncertainties in low-cloud responses. It therefore appears obvious that
348 constraining how low clouds respond to global warming would very likely reduce the spread
349 of climate sensitivity among models, and that many emergent constraints on ECS can be un-
350 derstood as encoding properties of shortwave low-cloud feedbacks [*Qu et al.*, 2018]. Con-

351 versely, emergent constraints that are only indirectly related to clouds should be viewed with
352 caution.

353 A number of studies have highlighted relationships between low-cloud amount changes
354 under global warming and modeled variations of low clouds with changes in specific mete-
355 orological conditions, such as surface temperature, inversion strength, subsidence [*Qu et al.*,
356 2013, 2015; *Myers and Norris*, 2013, 2015; *Brient and Schneider*, 2016]. These studies sug-
357 gest two robust low-cloud feedbacks: a decrease in low-cloud amount with surface warming
358 (related to increasing boundary-layer ventilation) and an increase of low-cloud amount with
359 inversion strengthening (related to a reduced cloud-top entrainment of dry air). Models show
360 that the former feedback mostly dominates the latter under a global warming, and that the
361 more realistic models exhibit larger low-cloud feedback [*Qu et al.*, 2013, 2015; *Brient and*
362 *Schneider*, 2016]. The convergence of studies using different methodologies and different
363 observations increases our confidence that low-cloud amount feedback more likely lie in the
364 upper range of simulated estimates.

365 Given that the strength of low-cloud amount feedback strongly correlates with ECS,
366 temporal variations in low-cloud albedo appears as a credible metric for constraining ECS.
367 Observations suggests most likely ECS estimates around 4 K, roughly identical for differ-
368 ent temporal frequencies of cloud variations [*Zhai et al.*, 2015; *Brient and Schneider*, 2016].
369 Despite this robustness, these conclusions are sensitive to the short time period (around a
370 decade) over which observations provide accurate enough characteristics of low-clouds.
371 Low-cloud short-term variations might only partly reflect long-term feedback [*Zhou et al.*,
372 2015], likely because of slow evolving spatial pattern of surface temperature that delay inver-
373 sion changes and cloud feedback in subsiding regions [*Ceppi and Gregory*, 2017; *Andrews*
374 *et al.*, 2018].

375 Although low-cloud amount feedback is the main driver of uncertainties in climate sen-
376 sitivity, other cloud responses contribute to the spread as well. One of them is the low-cloud
377 optical feedback, which is defined by the radiative influence of changes in optical properties
378 given unchanged cloud amount and altitude. *Gordon and Klein* [2014] show that the natu-
379 ral variability of mid-latitude cloud optical depth with temperature is well correlated with its
380 changes with global warming. This relationship stems from fundamental thermodynamics,
381 i.e. the increase in water content with warming [*Betts and Harshvardhan*, 1987], and mi-
382 crophysical changes, i.e. the relative increase of liquid content relative to ice within clouds

383 [Mitchell *et al.*, 1989]. This supports a robust negative cloud optical feedback with warm-
384 ing. Observations suggest that models are usually biased high, thus overestimating the nega-
385 tive mid-latitude low-cloud optical feedback. A misrepresentation of mixed-phase processes
386 within these extratropical clouds may explain this bias [McCoy *et al.*, 2015], which has been
387 pinpointed as being a key driver of differences in cloud feedback and climate sensitivity esti-
388 mates [Tan *et al.*, 2016].

389 The cloud altitude response to global warming may also amplify the original warming,
390 and models continue to disagree on the strength of this feedback [Zelinka *et al.*, 2013]. Phys-
391 ical mechanisms of high cloud elevation with warming are well understood [Hartmann and
392 Larson, 2002], making high-cloud altitude feedback very likely positive. Yet it remains un-
393 known to what extent the high-cloud amount and the high-cloud optical depth change with
394 warming. These changes are related to upper-tropospheric divergence and microphysics,
395 which need to be constrained individually. Some studies suggest a decreasing high-cloud
396 amount due to more efficient large-scale organization with warming [e.g. Bony *et al.*, 2016],
397 which point the way towards mechanistic emergent constraints on high-cloud feedback.

398 Better constraining cloud feedback will therefore very likely lead to better constraints
399 on the equilibrium climate sensitivity. This target should be addressed through process-based
400 understanding of individual cloud changes, such as how the relative coverage of tropical
401 low clouds evolves, how high cloud fraction change as they move upward, or to what extent
402 small-scale microphysical changes perturb the climate system. Merging realistic estimates of
403 these feedbacks would give a step forward for accurately constraining the equilibrium climate
404 sensitivity.

405 **6 Constraining Climate Changes**

406 In the last decade, the concept of emergent constraints has begun to be widely applied
407 in different branches of climate science that allowed constraining uncertain responses of the
408 Earth system, such as the hydrological cycle, the carbon cycle, or various regional changes.

409 **6.1 The hydrological cycle**

410 Uncertainties in the response of precipitation to global warming are important and
411 remain to be narrowed. Increasing the confidence in precipitation changes would provide
412 important benefits for regional climate projections and risk assessment [Christensen *et al.*,

413 2013]. Links between natural variability of extreme precipitation and temperature offer possible
414 observational constraints for changes in climate extremes, especially because the underlying
415 physical mechanisms are relatively well understood [O’Gorman and Schneider, 2008].
416 These constraints usually suggest a strong intensification of heavy rainfall with warming
417 [O’Gorman, 2012; Borodina et al., 2017]. Changes in the hydrological cycle can partly be
418 attributed to changes in the clear-sky shortwave absorption, which is related to models’ radiative
419 transfer parameterizations [DeAngelis et al., 2015]. That emphasis on processes that
420 explain inter-model difference in the predictor might lead to targeted model development for
421 narrowing climate projections.

422 **6.2 The carbon cycle**

423 A second topic that has also received great emphasis is the sensitivity of the carbon
424 cycle to climate change. Cox et al. [2013] found a robust relationship that links interannual
425 co-variations between tropical temperature and carbon release into the atmosphere (the predictor)
426 and the weakening in carbon storage under global warming. Observations highlight
427 that most climate models overestimate the present-day sensitivity of land CO₂ changes, suggesting
428 a too strong weakening of the CO₂ tropical land storage with climate change (Table 1).
429 This constraint has been confirmed by following analysis [Wang et al., 2014; Wenzel
430 et al., 2014]. Additional studies have aimed to constrain other aspects of the climate-carbon
431 cycle feedback, such as the land photosynthesis [Wenzel et al., 2016], sinks and sources of
432 carbon dioxide [Hoffman et al., 2014; Winkler et al., 2019], and the tropical ocean primary
433 production [Kwiatkowski et al., 2017].

434 **6.3 Geoengineering**

435 Constraining uncertainties in geoengineering simulations has also been addressed.
436 Inter-model differences in the climate response to an artificial increase of sulfate concentrations
437 are correlated to inter-model differences in the simulated cooling by past volcanic eruptions
438 [Plazzotta et al., 2018]. Physical assumptions underlying this relationship consists
439 in assuming that volcanic eruptions can be understood as an analogue of solar radiation management
440 [Trenberth and Dai, 2007]. Observations from satellites suggest that models overestimate
441 the cooling by volcanic eruptions, thus overestimating the potential cooling effect by
442 an addition of aerosols in the stratosphere.

6.4 Regional climate changes

While most emergent constraints focus on global scales, several aim to better understand and constrain regional climate changes. So far these studies mostly focus on extratropical climate responses, as was the case for the pioneering work of *Hall and Qu* [2006]. Attempts in constraining changes of extreme temperature have recently showed that models slightly overestimate the increasing frequency of heat extremes with global warming in Europe and North America [*Donat et al.*, 2018], in relation with a too strong soil drying [*Douville and Plazzotta*, 2017]. Changes in the extratropical circulation have also been studied. Models show a robust poleward shift of the South Hemisphere jet with global warming, and are uncertain about the sign of the North Hemisphere jet shift. Emergent constraints and statistical inference suggest that models overestimate the southern hemispheric poleward shift [*Kidston and Gerber*, 2010; *Simpson and Polvani*, 2016] and predict that the northern hemisphere jet will likely move poleward [*Gao et al.*, 2016]. Finally, a number of studies aim to constrain changes over the Arctic region. They show that a majority of models delays the year when summertime sea-ice cover would likely disappear [*Boé et al.*, 2009; *Massonnet et al.*, 2012] and slightly overestimates the strength of the polar amplification [*Bracegirdle and Stephenson*, 2013].

Regional emergent constraints remain rare, which reduce the ability to compare metrics and observations to one another. Results are thus not robust yet, and should be viewed with caution. However, knowing the large uncertainties underlying regional climate projections and the advantages local populations will get from better model projections [*Christensen et al.*, 2013], I expect to see numerous new emergent constraints aimed to narrow uncertainties in regional climate changes in the near future. Nevertheless, this should be addressed through rigorous physical understanding given the numerous multi-scale interactions and adjustments that induce regional differences.

6.5 Paleoclimate

The sensitivity of global-mean temperature to Earth's orbital variations and/or CO₂ natural changes might be considered an analogue of the warming induced by the artificial CO₂ increase, i.e. the climate sensitivity to past climate change an analogue to the equilibrium climate sensitivity (as defined by *Gregory et al.* [2004]). When imposing such past variations, climate models suggest different responses in the strength of global-mean cool-

474 ing that may be related to the spread in ECS. For instance, *Hargreaves et al.* [2012] shows
475 that the simulated global-mean cooling during the Last Glacial Maximum (LGM, 19-23 ka
476 before present) is inversely correlated with ECS in CMIP3 models. Constraining the LGM
477 cooling from proxy data yields a most likely climate sensitivity around 2.3 K, which is lower
478 than emergent constraints based on the mean state or variability (Table 1). A number of crit-
479 icisms may arise from this inference, such as the realism of the LGM CMIP simulations, un-
480 certainties underlying proxies used for observational reference, and the use of paleoclimates
481 as a surrogate for global warming (differences in temperature patterns, albedo feedback etc.).
482 These uncertainties may partly explain the frequent weak correlations found between paleo-
483 climate indices and climate projections, and the difficulty in narrowing the spread in models'
484 climate sensitivity estimates from paleoclimate-based emergent constraints [*Schmidt et al.*,
485 2013; *Harrison et al.*, 2015].

486 **7 Do emergent constraints narrow the spread of climate sensitivity so far?**

487 Table 1 lists 11 emergent constraints that provide best estimates for climate sensitivity
488 using various predictors (without paleoclimate indexes). Here I inquire whether taken all to-
489 gether they reduce the raw model uncertainty (e.g., 3.4 ± 0.8 K for CMIP5 models). For that
490 purpose, I build a normal distribution for each of 11 ECS emergent constraints listed on ta-
491 ble 1, with mean value and standard deviation taken from the original studies. These values
492 correspond to moments provided by the authors if available, or estimated from the emergent
493 relationship otherwise (and thus correspond to a raw estimate of the real posterior estimate).
494 I attribute each distribution an equal weight of 1/11, which assume that emergent constraints
495 are independent with each other and equally valuable. Finally, note that the width to each
496 normal distribution is strongly influenced by uncertainties underlying the statistical inference,
497 which differ across studies, and observation uncertainties, which might be sometimes under-
498 estimated [e.g. *Volodin*, 2008]. Figure 3 shows all individual distributions, the prior distri-
499 bution for CMIP models and the combined posterior distribution. It shows that this posterior
500 distribution is really close to the prior distributions, yet slightly skewed toward higher ECS
501 values (explained by the majority of emergent constraints that suggest higher-than-average
502 ECS values). However, the disagreement between emergent constraints and their large uncer-
503 tainties do not significantly narrow the original spread in ECS. This suggests that emergent
504 constraints need to be better assessed through a verification of physical mechanisms explain-
505 ing the relationship [*Caldwell et al.*, 2018; *Hall et al.*, 2019]. This would give the ability to

weight each emergent constraint and provide a better posterior distribution allowing to trustingly narrow the spread in future climate changes. Finally, statistical inference and observational uncertainties need to be better informed for cross-validation of posterior estimates.

8 Conclusions

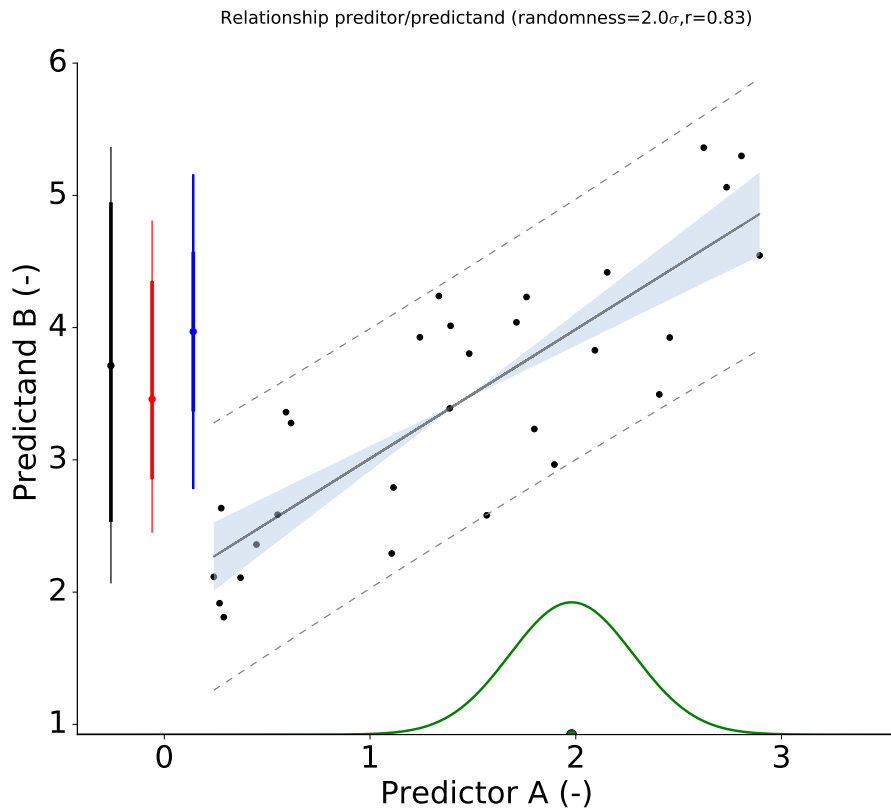
This paper presents the concept of emergent constraints, a methodology that aim to narrow uncertainties in climate change projections by identifying a link between them and the inter-model spread in an observable predictor. In the last decade, the number of studies that used this framework grew significantly and provided constraints on various climate projections (an exhaustive list of published emergent constraints is presented on table 1). The majority focused on narrowing uncertainties in equilibrium climate sensitivity, cloud feedback, and carbon cycle feedbacks. Others focused on components of the climate system in relation with changes of the hydrological cycle, the cryosphere, or the dynamical shift of mid-latitude jet, among others. Predictors can be gathered in two main categories: natural variations of the variable of interest with temperature variability or a mean feature of the climate system. This sometimes leads to metrics not directly related to the considered predictand. Physical explanations for emergent constraints are diverse and thus a majority of them remain to be confirmed. Weighting the credibility of emergent constraints would very likely increase the confidence in posterior estimates aimed to narrow the spread in climate projections.

The diversity of emergent constraints highlight the commitment of the climate community to narrowing uncertainties in climate projections. This interest will likely continue to grow since a large number of changes in climate phenomena simulated by models remain uncertain, even when fundamental mechanisms are relatively well understood (e.g., changes in monsoons, heat waves, cyclones). The emergent constraint framework can thus be seen as a new promising way to evaluate climate models [Eyring *et al.*, 2019; Hall *et al.*, 2019], especially with the upcoming CMIP6 project that will very likely boost this enthusiasm. However, this calls for robust statistical inference for providing credible uncertainty reductions. In that purpose, the code used for quantifying inference and uncertainties in Figure 4 with two different methods is shared¹. Quantifying posterior posterior estimates with different frameworks (either from inference or model weighting) allows testing the confidence in

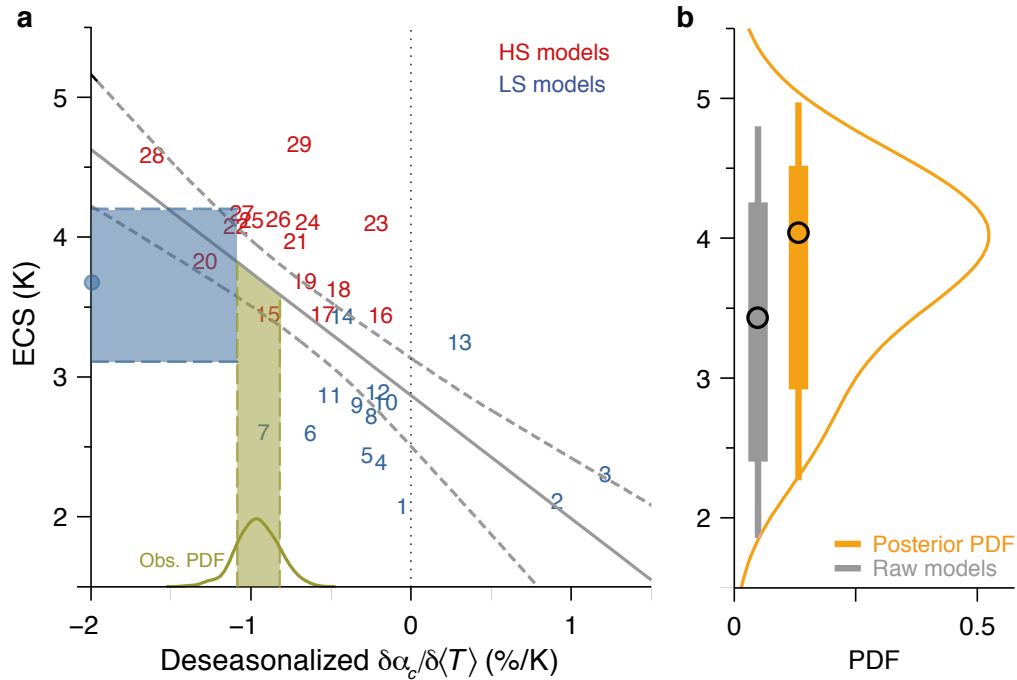
¹ https://github.com/florentbrient/emergent_constraint

536 predictions. Further improvements would consists in continuing testing difference statisti-
537 cal inference procedures and building multi-predictor weighting method to benefit from the
538 number of proposed emergent constraints .

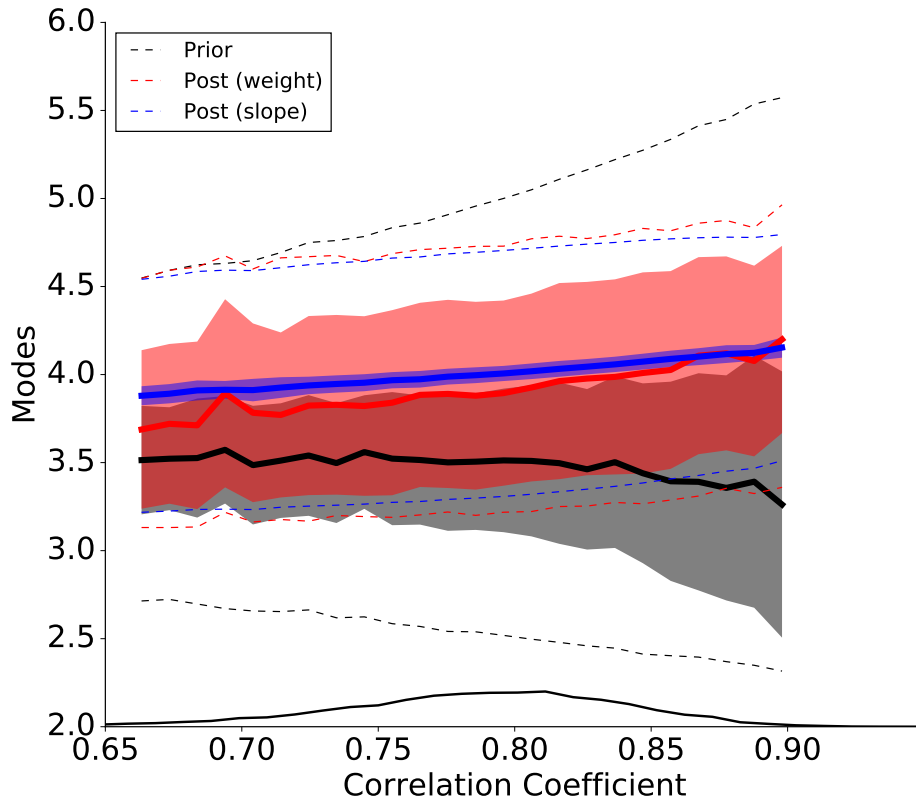
539 Beyond the post-facto model evaluation, it will finally be interesting to see whether
540 new climate models take advantage of emergent constraints to improve their simulation of
541 present-day climate and to reduce uncertainties in future projections.



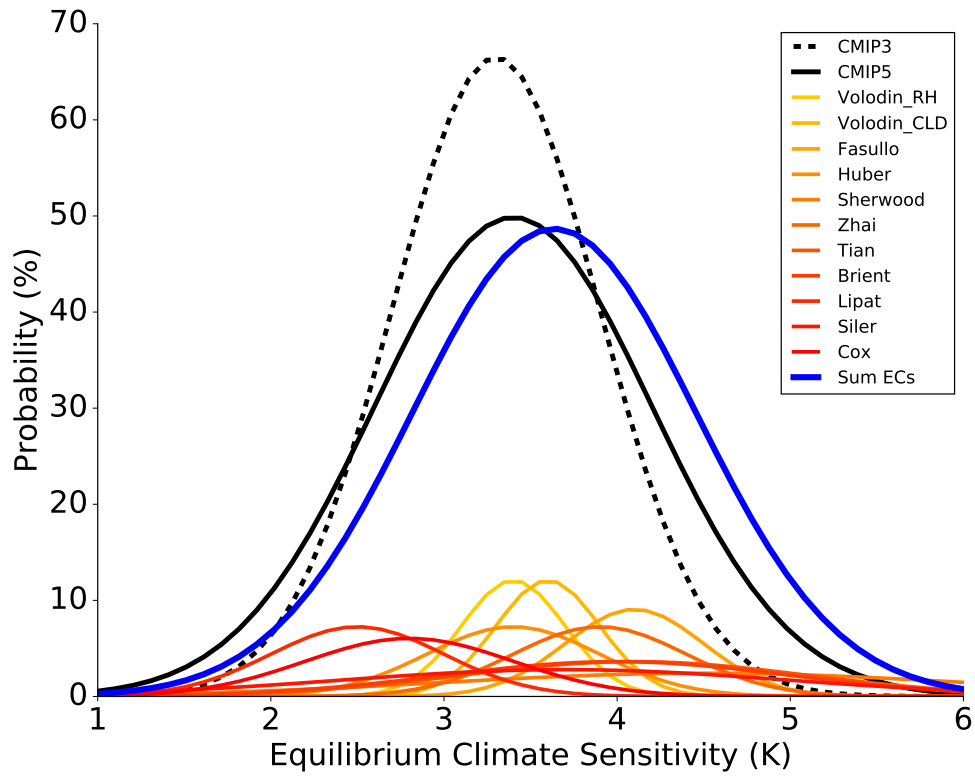
542 **Figure 1.** Idealized relationship between a predictor and a predictand. The 29 models (dots) are associated
 543 with arbitrary values of the predictor A (x here between 0 and 3). The predictand B on the y-axis follows
 544 the idealized relationship ($y' = ax + b$ with $a=1.$ and $b=2.$) plus a random deviation Δ following a normal
 545 distribution with $\sigma=2$ (such as $y = y' + \Delta(y')$). The dashed lines and blue shades represent the 90% prediction
 546 limits and the 90% confidence limits of the slope respectively. The green distribution on the x-axis represents
 547 an idealized observed distribution of the predictor, assuming a normal distribution (here with $\mu=1.98$ and
 548 $\sigma=0.3$). Prior and posterior distributions of the predictand are represented as vertical lines on the left part,
 549 with mode (circle), 66% (thick) and 90% (thin) confidence intervals. Black lines represent the prior distri-
 550 bution, red lines represent the posterior distribution obtained by a weighted average of the climate models
 551 through a Kullback-Leibler divergence and blue lines are the one inferred using the slope and its uncertainties.
 552 In that randomly generated example, posterior estimates are sensitive to the way inference is computed.



553 **Figure 2.** (a) Scatterplot of ECS vs deseasonalized covariance of marine tropical low-cloud (TLC) re-
 554 flectance α_c with surface temperature T in CMIP5 models (numbered in order of increasing ECS). Gray
 555 lines represent a robust regression line (solid), with the 90% confidence interval of the fitted values (dashed)
 556 estimated by a bootstrap procedure. The green line at the lower axis indicates the PDF of the deseasonalized
 557 TLC reflectance variation with surface temperature inferred from observations. The vertical green band in-
 558 dicates the 66% band of the observations. The blue circle and horizontal band shows the mode and the likely
 559 (66%) ECS range inferred from a linear regression procedure respectively, taking into account uncertainties
 560 estimated by bootstrapping predictions with estimating regression models. (b) Posterior PDF of ECS (orange)
 561 obtained by a weighted average of the climate models, given the observations. The bars with circles represent
 562 the mode and confidence intervals (66% and 90%) implied by the posterior (orange) PDF and the prior (gray)
 563 PDF. Adapted from *Brient and Schneider* [2016].



564 **Figure 3.** Relationship between modes and correlation coefficient (r) of 10^4 randomly-generated emergent
 565 constraints, as the example shown on Figure 1. Thick lines, dashed lines and shades represent the average
 566 mode, the average 66% confidence interval and the standard deviation of mode across the set of emergent
 567 relationship. Characteristics of the prior distributions are represented in black color. Posterior estimates using
 568 the slope inference or the weighting averaging are represented in blue and red respectively, using an idealized
 569 observed distribution of the predictor as defined on Figure 1. The probability density function of correlation
 570 coefficients is shown as a thin black line on the x-axis. This figure shows that average modes and confidence
 571 intervals remain independent of the inference method, but the uncertainty of the mode value is larger for the
 572 weighting method.



573 **Figure 4.** Probability density functions (PDFs) of equilibrium climate sensitivity (ECS) from the original
 574 inter-model distribution (CMIP3 and CMIP5 models) and based on posterior distributions derived from 11
 575 emergent constraints listed on table 1. Each emergent constraint PDF is defined as a normal distribution with
 576 mean and standard deviation listed on table 1. The blue line is the ECS distribution covered by all equally-
 577 weighted emergent constraint distributions.

578 **Table 1.** List of 44 published emergent constraints, the predictand they constrain, the original and the con-
 579 strained ranges. Mean and standard deviations of prior and posterior estimates are listed when available. The
 580 * sign signifies that the moments of the distribution are not directly quantified in the reference paper but de-
 581 rived from their emergent relationship and the observational constraint, and thus should be understood only as
 582 qualitative assessment.

Reference	Predictand	Original	Constrained
<i>Covey et al.</i> [2000] <i>Volodin</i> [2008] (RH) <i>Volodin</i> [2008] (Cloud) <i>Trenberth and Fasullo</i> [2010] <i>Huber et al.</i> [2011] <i>Fasullo and Trenberth</i> [2012] <i>Sherwood et al.</i> [2014] <i>Su et al.</i> [2014] <i>Zhai et al.</i> [2015] <i>Tian</i> [2015] <i>Brient and Schneider</i> [2016] <i>Lipat et al.</i> [2017] <i>Siler et al.</i> [2018] <i>Cox et al.</i> [2018]	ECS (K)	3.4±0.8 3.3±0.6 3.4±0.8	– 3.4±0.3 3.6±0.3 >4.0 3.4±0.6 4.1±0.4* 4.5±1.5* >3.4 3.9±0.5 4.1±1.0* 4.0±1.0* 2.5±0.5* 3.7±1.3 2.8±0.6
<i>Qu et al.</i> [2013] <i>Gordon and Klein</i> [2014] <i>Brient and Schneider</i> [2016]	Low-cloud amount feedback (%/K) Low-cloud optical depth feedback (K ⁻¹) Low-cloud albedo change (%/K)	-1.0±1.5 0.04±0.03 -0.12±0.28	– – -0.4±0.4*
<i>Siler et al.</i> [2018]	Global cloud feedback (%/K)	0.43±0.30	0.58±0.31
<i>Allen and Ingram</i> [2002] <i>O’Gorman</i> [2012] <i>DeAngelis et al.</i> [2015] <i>Li et al.</i> [2017]	Global-mean precipitation Tropical precipitation extremes (%/K) Clear-sky shortwave absorption (W/m ² /K) Indian Monsoon rainfall changes (%/K)	– 2-23 0.8±0.3 +6.5±5.0	– 6-14 1.0±0.1 +3.5±4.0
<i>Cox et al.</i> [2013] <i>Wang et al.</i> [2014] <i>Wenzel et al.</i> [2014] <i>Hoffman et al.</i> [2014] <i>Wenzel et al.</i> [2016] <i>Kwiatkowski et al.</i> [2017] <i>Winkler et al.</i> [2019]	Tropical land carbon release (GtC/K) CO ₂ concentration in 2100 (ppm) Gross Primary Productivity (%) Tropical ocean primary production (%/K) Gross Primary Production (PgC/yr)	69±39 79±43 49±40 980±161 +34±15 -4.0±2.2 2.1±1.9	53±17 70±45* 44±14 947±35 +37±9 -3.0±1.0 3.4±0.2
<i>Plazzotta et al.</i> [2018]	Global-mean cooling by sulfate (K/W/m ²)	0.54±0.33	0.44±0.24
<i>Hall and Qu</i> [2006] <i>Qu and Hall</i> [2014] <i>Boé et al.</i> [2009] <i>Massonnet et al.</i> [2012] <i>Bracegirdle and Stephenson</i> [2013]	Snow-albedo feedback (%/K) Remaining Arctic sea-ice cover in 2040 (%) Years of summer Arctic ice free Arctic warming (°C)	-0.8±0.3 -0.9±0.3 67±20* [2029-2100+] ~2.78	-1.0±0.1* -1.0±0.2* 37±10* [2041-2060] <2.78
<i>Kidston and Gerber</i> [2010] <i>Simpson and Polvani</i> [2016] <i>Gao et al.</i> [2016] <i>Gao et al.</i> [2016] <i>Douville and Plazzotta</i> [2017] <i>Lin et al.</i> [2017] <i>Donat et al.</i> [2018]	Shift of the South Hemispheric Jet (°) Shift of the North Hemispheric Jet (°) Summer midlatitude soil moisture Summer US temperature changes (°C) Frequency of heat extremes (-)	-1.8±0.7 ~-3 ~0 ~+1.5 – +6.0±0.8 –	-0.9±0.6 ~-0.5* (Winter) ~-2 (Winter) ~-1 (Spring) – +5.2±1.0* –
<i>Hargreaves et al.</i> [2012] <i>Schmidt et al.</i> [2013]	ECS (K)	3.1±0.9 3.3±0.8	2.3±0.9 3.1±0.7

Acknowledgments

This work received funding from grant HIGH-TUNE ANR-16-CE01-0010. I thank Tapio Schneider for the number of discussions we had on this topic, and for sharing his thoughts on statistical inference. I also thank Ross Dixon for interesting discussions and for proof-reading the manuscript. Routines for the randomly-generated relationship and the statistical inferences are available on the Github website (https://github.com/florentbrient/emergent_constraint/).

References

- Adam, O., T. Schneider, F. Brient, and T. Bischoff (2016), Relation of the double-ITCZ bias to the atmospheric energy budget in climate models, *Geophys Res Lett*, 43(14), 7670–7677.
- Adam, O., T. Schneider, and F. Brient (2017), Regional and seasonal variations of the double-itz bias in cmip5 models, *Clim. Dyn.*, pp. 1–17.
- Allen, M. R., and W. J. Ingram (2002), Constraints on future changes in climate and the hydrologic cycle, *Nature*, 419, 224–231.
- Andrews, T., J. M. Gregory, D. Paynter, L. G. Silvers, C. Zhou, T. Mauritsen, M. J. Webb, K. C. Armour, P. M. Forster, and H. Titchner (2018), Accounting for changing temperature patterns increases historical estimates of climate sensitivity, *Geophys Res Lett*, 45(16), 8490–8499.
- Betts, A. K., and Harshvardhan (1987), Thermodynamic constraint on the cloud liquid water feedback in climate models, *J. Geophys. Res.*, 92, 8483–8485.
- Boé, J., A. Hall, and X. Qu (2009), September sea-ice cover in the arctic ocean projected to vanish by 2100, *Nature Geoscience*, 2(5), 341.
- Bony, S., R. Colman, V. Kattsov, R. Allan, C. Bretherton, J.-L. Dufresne, A. Hall, S. Hallette, M. Holland, W. Ingram, D. Randall, B. Soden, G. Tselioudis, and M. Webb (2006), How well do we understand and evaluate climate change feedback processes?, *J Clim*, 19(15), 3445–3482.
- Bony, S., G. Bellon, D. Klocke, S. Sherwood, S. Fermepin, and S. Denvil (2013), Robust direct effect of carbon dioxide on tropical circulation and regional precipitation, *Nature Geosciences*, 6(6), 447–451.
- Bony, S., B. Stevens, D. Coppin, T. Becker, K. A. Reed, A. Voigt, and B. Medeiros (2016), Thermodynamic control of anvil cloud amount, *Proc. Nat. Ac. Sci.*, 113(32), 8927–8932.

- 615 Borodina, A., E. M. Fischer, and R. Knutti (2017), Models are likely to underestimate in-
616 crease in heavy rainfall in the extratropical regions with high rainfall intensity, *Geophys*
617 *Res Lett*, *44*(14), 7401–7409.
- 618 Bracegirdle, T. J., and D. B. Stephenson (2013), On the robustness of emergent constraints
619 used in multimodel climate change projections of arctic warming, *J Clim*, *26*(2), 669–678.
- 620 Brient, F., and S. Bony (2013), Interpretation of the positive low-cloud feedback predicted by
621 a climate model under global warming, *Clim. Dyn.*, *40*(9-10), 2415–2431.
- 622 Brient, F., and T. Schneider (2016), Constraints on climate sensitivity from space-based mea-
623 surements of low-cloud reflection, *J Clim*, *29*(16), 5821–5835.
- 624 Brient, F., T. Schneider, Z. Tan, S. Bony, X. Qu, and A. Hall (2016), Shallowness of tropical
625 low clouds as a predictor of climate models’ response to warming, *Clim. Dyn.*, pp. 1–17.
- 626 Burnham, K. P., and D. R. Anderson (2010), *Model Selection and Multimodel Inference: A*
627 *Practical Information-Theoretic Approach*, 2nd ed., Springer, New York, NY.
- 628 Caldwell, P. M., C. S. Bretherton, M. D. Zelinka, S. A. Klein, B. D. Santer, and B. M.
629 Sanderson (2014), Statistical significance of climate sensitivity predictors obtained by data
630 mining, *Geophys Res Lett*, *41*(5), 1803–1808.
- 631 Caldwell, P. M., M. D. Zelinka, and S. A. Klein (2018), Evaluating emergent constraints on
632 equilibrium climate sensitivity, *J Clim*, *31*(10), 3921–3942.
- 633 Ceppi, P., and J. M. Gregory (2017), Relationship of tropospheric stability to climate sen-
634 sitivity and earth’s observed radiation budget, *Proc. Nat. Ac. Sci.*, *114*(50), 13,126–
635 13,131.
- 636 Ceppi, P., F. Brient, M. D. Zelinka, and D. L. Hartmann (2017), Cloud feedback mechanisms
637 and their representation in global climate models, *WIREs*.
- 638 Cess, R., M. H. Zhang, W. J. Ingram, G. L. Potter, V. Alekseev, H. W. Barker, E. Cohen-
639 Solal, R. A. Colman, D. A. Dazlich, A. D. D. Genio, M. R. Dix, V. Dymnikov, M. Esch,
640 L. D. Fowler, J. R. Fraser, V. Galin, W. L. Gates, J. J. Hack, J. T. Kiehl, H. L. Treut, K. K.-
641 W. Lo, B. J. McAvaney, V. P. Meleshko, J.-J. Morcrette, D. A. Randall, E. Roeckner, J.-
642 F. Royer, M. E. Schlesinger, P. V. Sporyshev, B. Timbal, K. E. Taylor, E. M. Volodin,
643 W. Wang, and R. T. Wetherald (1996), Cloud feedback in atmospheric general circulation
644 models: An update, *J. Geophys. Res.*, *101*, 12,791–12,794.
- 645 Cess, R. D., G. Potter, J. Blanchet, G. Boer, A. Del Genio, M. Deque, V. Dymnikov, V. Galin,
646 W. Gates, S. Ghan, et al. (1990), Intercomparison and interpretation of climate feed-
647 back processes in 19 atmospheric general circulation models, *J. Geophys. Res.*, *95*(16),

648 601,216.

649 Charney, J. G., A. Arakawa, D. J. Baker, B. Bolin, R. E. Dickinson, R. M. Goody, C. E.

650 Leith, H. M. Stommel, and C. I. Wunsch (1979), *Carbon dioxide and climate : a scien-*

651 *tific assessment*, 33 pp., National Academy of Sciences.

652 Christensen, J. H., K. K. Kanikicharla, G. Marshall, and J. Turner (2013), Climate phenom-

653 ena and their relevance for future regional climate change, in *Climate change 2013: the*

654 *physical science basis. Contribution of Working Group I to the Fifth Assessment Report of*

655 *the Intergovernmental Panel on Climate Change*, Cambridge University Press.

656 Covey, C., A. Abe-Ouchi, G. Boer, B. Boville, U. Cubasch, L. Fairhead, G. Flato, H. Gor-

657 don, E. Guilyardi, X. Jiang, et al. (2000), The seasonal cycle in coupled ocean-atmosphere

658 general circulation models, *Clim. Dyn.*, 16(10-11), 775–787.

659 Cox, P. M., D. Pearson, B. B. Booth, P. Friedlingstein, C. Huntingford, C. D. Jones, and

660 C. M. Luke (2013), Sensitivity of tropical carbon to climate change constrained by carbon

661 dioxide variability, *Nature*, 494(7437), 341.

662 Cox, P. M., C. Huntingford, and M. S. Williamson (2018), Emergent constraint on equilib-

663 rium climate sensitivity from global temperature variability, *Nature*, 553(7688), 319.

664 DeAngelis, A., X. Qu, M. Zelinka, and A. Hall (2015), An observational radiative constraint

665 on hydrologic cycle intensification, *Nature*, 528(7581), 249–253.

666 Dee, D., S. Uppala, A. Simmons, P. Berrisford, P. Poli, S. Kobayashi, U. Andrae, M. Bal-

667 maseda, G. Balsamo, P. Bauer, et al. (2011), The ERA-Interim reanalysis: Configuration

668 and performance of the data assimilation system, *Quart. J. Roy. Meteor. Soc.*, 137(656),

669 553–597.

670 Donat, M. G., A. J. Pitman, and O. Angéilil (2018), Understanding and reducing future un-

671 certainty in midlatitude daily heat extremes via land surface feedback constraints, *Geophys*

672 *Res Lett*, 45(19), 10–627.

673 Douville, H., and M. Plazzotta (2017), Midlatitude summer drying: An underestimated

674 threat in cmip5 models?, *Geophys Res Lett*, 44(19), 9967–9975.

675 Dufresne, J.-L., and S. Bony (2008), An assessment of the primary sources of spread of

676 global warming estimates from coupled atmosphere-ocean models, *J Clim*, 21(19), 5135–

677 5144.

678 Eyring, V., P. M. Cox, G. M. Flato, P. J. Gleckler, G. Abramowitz, P. Caldwell, W. D.

679 Collins, B. K. Gier, A. D. Hall, F. M. Hoffman, et al. (2019), Taking climate model evalua-

680 tion to the next level, *Nature Climate Change*, p. 1.

- 681 Fasullo, J. T., and K. E. Trenberth (2012), A less cloudy future: The role of subtropical sub-
682 sidence in climate sensitivity, *Science*, 338(6108), 792–794.
- 683 Flato, G., J. Marotzke, B. Abiodun, P. Braconnot, S. C. Chou, W. Collins, P. Cox, F. Dri-
684 ouech, S. Emori, V. Eyring, et al. (2013), Evaluation of climate models, in *Climate*
685 *Change 2013: The Physical Science Basis. Contribution of Working Group I to the Fifth*
686 *Assessment Report of the Intergovernmental Panel on Climate Change*, pp. 741–866, Cam-
687 bridge University Press.
- 688 Găinușă-Bogdan, A., P. Braconnot, and J. Servonnat (2015), Using an ensemble data set of
689 turbulent air-sea fluxes to evaluate the ipsl climate model in tropical regions, *J. Geophys.*
690 *Res.*, 120(10), 4483–4505.
- 691 Gao, Y., J. Lu, and L. R. Leung (2016), Uncertainties in projecting future changes in atmo-
692 spheric rivers and their impacts on heavy precipitation over europe, *Journal of Climate*,
693 29(18), 6711–6726.
- 694 Gordon, N. D., and S. A. Klein (2014), Low-cloud optical depth feedback in climate models,
695 *J. Geophys. Res.*, 119(10), 6052–6065.
- 696 Gregory, J., W. Ingram, M. Palmer, G. Jones, P. Stott, R. Thorpe, J. Lowe, T. Johns, and
697 K. Williams (2004), A new method for diagnosing radiative forcing and climate sensi-
698 tivity, *Geophys Res Lett*, 31(3), L03,205.
- 699 Hall, A., and S. Manabe (1999), The role of water vapour feedback in unperturbed climate
700 variability and global warming, *J Clim*, 12, 2327–2346.
- 701 Hall, A., and X. Qu (2006), Using the present-day seasonal cycle to constrain climate sen-
702 sitivity: A case study of snow albedo feedback, *Geophys Res Lett*, 33, 1550–1568, doi:
703 10.1029/2005GL025127.
- 704 Hall, A., P. Cox, C. Huntingford, and S. Klein (2019), Progressing emergent constraints on
705 future climate change, *Nat. Clim. Change*, p. 1.
- 706 Hargreaves, J. C., J. D. Annan, M. Yoshimori, and A. Abe-Ouchi (2012), Can the last glacial
707 maximum constrain climate sensitivity?, *Geophys Res Lett*, 39(24).
- 708 Harrison, S. P., P. Bartlein, K. Izumi, G. Li, J. Annan, J. Hargreaves, P. Braconnot, and
709 M. Kageyama (2015), Evaluation of cmip5 palaeo-simulations to improve climate pro-
710 jections, *Nature Climate Change*, 5(8), 735.
- 711 Hartmann, D. L., and K. Larson (2002), An important constraint on tropical cloud-climate
712 feedback, *Geophys Res Lett*, 29, 1951–1954.

- 713 Hoffman, F. M., J. T. Randerson, V. K. Arora, Q. Bao, P. Cadule, D. Ji, C. D. Jones,
714 M. Kawamiya, S. Khatiwala, K. Lindsay, et al. (2014), Causes and implications of per-
715 sistent atmospheric carbon dioxide biases in earth system models, *Journal of Geophysical*
716 *Research: Biogeosciences*, *119*(2), 141–162.
- 717 Huber, M., I. Mahlstein, M. Wild, J. Fasullo, and R. Knutti (2011), Constraints on climate
718 sensitivity from radiation patterns in climate models, *J Clim*, *24*(4), 1034–1052.
- 719 Hwang, Y.-T., and D. M. Frierson (2013), Link between the double-intertropical convergence
720 zone problem and cloud biases over the southern ocean, *Proc. Nat. Ac. Sci.*, *110*(13),
721 4935–4940.
- 722 Kamae, Y., H. Shiogama, M. Watanabe, T. Ogura, T. Yokohata, and M. Kimoto (2016),
723 Lower-tropospheric mixing as a constraint on cloud feedback in a multiparameter multi-
724 physics ensemble, *J Clim*, *29*(17), 6259–6275.
- 725 Kidston, J., and E. Gerber (2010), Intermodel variability of the poleward shift of the austral
726 jet stream in the cmip3 integrations linked to biases in 20th century climatology, *Geophys*
727 *Res Lett*, *37*(9).
- 728 Klein, S. A., and A. Hall (2015), Emergent constraints for cloud feedbacks, *Curr. Clim.*
729 *Change Rep.*, *1*(4), 276–287.
- 730 Knutti, R., D. Masson, and A. Gettelman (2013), Climate model genealogy: Generation
731 CMIP5 and how we got there, *Geophys Res Lett*, *40*(6), 1194–1199.
- 732 Kwiatkowski, L., L. Bopp, O. Aumont, P. Ciais, P. M. Cox, C. Laufkötter, Y. Li, and
733 R. Séférian (2017), Emergent constraints on projections of declining primary production
734 in the tropical oceans, *Nat. Clim. Change*, *7*(5), 355.
- 735 Li, G., S.-P. Xie, C. He, and Z. Chen (2017), Western pacific emergent constraint lowers pro-
736 jected increase in indian summer monsoon rainfall, *Nat. Clim. Change*, *7*(10), 708.
- 737 Lin, Y., W. Dong, M. Zhang, Y. Xie, W. Xue, J. Huang, and Y. Luo (2017), Causes of model
738 dry and warm bias over central us and impact on climate projections, *Nature communica-*
739 *tions*, *8*(1), 881.
- 740 Lipat, B. R., G. Tselioudis, K. M. Grise, and L. M. Polvani (2017), Cmp5 models' shortwave
741 cloud radiative response and climate sensitivity linked to the climatological hadley cell
742 extent, *Geophys Res Lett*, *44*(11), 5739–5748.
- 743 Masson, D., and R. Knutti (2011), Climate model genealogy, *Geophys Res Lett*, *38*(8).
- 744 Massonnet, F., T. Fichet, H. Goosse, C. M. Bitz, G. Philippon-Berthier, M. M. Hol-
745 land, and P.-Y. Barriat (2012), Constraining projections of summer arctic sea ice, *The*

- 746 *Cryosphere*, 6(6), 1383–1394.
- 747 McCoy, D. T., D. L. Hartmann, M. D. Zelinka, P. Ceppi, and D. P. Grosvenor (2015), Mixed-
748 phase cloud physics and southern ocean cloud feedback in climate models, *J. Geophys.*
749 *Res.*, 120(18), 9539–9554.
- 750 Meehl, G. A., G. Boer, C. Covey, M. Latif, and R. Stouffer (2000), The Coupled Model Inter-
751 comparison Project (CMIP), *Bull. Amer. Meteor. Soc.*, 81, 313–318.
- 752 Mitchell, J. F., C. Senior, and W. Ingram (1989), CO₂ and climate: a missing feedback?, *Na-*
753 *ture*, 341(6238), 132.
- 754 Morice, C. P., J. J. Kennedy, N. A. Rayner, and P. D. Jones (2012), Quantifying uncertainties
755 in global and regional temperature change using an ensemble of observational estimates:
756 The hadcrut4 data set, *J. Geophys. Res.*, 117(D8).
- 757 Myers, T. A., and J. R. Norris (2013), Observational evidence that enhanced subsidence re-
758 duces subtropical marine boundary layer cloudiness, *J Clim*, 26(19), 7507–7524.
- 759 Myers, T. A., and J. R. Norris (2015), On the relationships between subtropical clouds and
760 meteorology in observations and cmip3 and cmip5 models, *J Clim*, 28(8), 2945–2967.
- 761 O’Gorman, P. A. (2012), Sensitivity of tropical precipitation extremes to climate change,
762 *Nature Geoscience*, 5(10), 697–700.
- 763 O’Gorman, P. A., and T. Schneider (2008), The hydrological cycle over a wide range of cli-
764 mates simulated with an idealized GCM, *J Clim*, 21(15), 3815–3832.
- 765 Plazzotta, M., R. Séférian, H. Douville, B. Kravitz, and J. Tjiputra (2018), Land surface
766 cooling induced by sulfate geoengineering constrained by major volcanic eruptions, *Geo-*
767 *phys Res Lett*.
- 768 Qu, X., and A. Hall (2014), On the persistent spread in snow-albedo feedback, *Clim. Dyn.*,
769 42(1-2), 69–81.
- 770 Qu, X., A. Hall, S. A. Klein, and P. M. Caldwell (2013), On the spread of changes in marine
771 low cloud cover in climate model simulations of the 21st century, *Clim. Dyn.*, pp. 1–24.
- 772 Qu, X., A. Hall, S. A. Klein, and A. M. DeAngelis (2015), Positive tropical marine low-
773 cloud cover feedback inferred from cloud-controlling factors, *Geophys Res Lett*, 42.
- 774 Qu, X., A. Hall, A. M. DeAngelis, M. D. Zelinka, S. A. Klein, H. Su, B. Tian, and C. Zhai
775 (2018), On the emergent constraints of climate sensitivity, *J Clim*, 31(2), 863–875.
- 776 Rossow, W. B., and R. A. Schiffer (1999), Advances in understanding clouds from ISCCP,
777 *Bull. Amer. Meteor. Soc.*, 80, 2261–2287.

- 778 Sanderson, B. M., R. Knutti, and P. Caldwell (2015), A representative democracy to reduce
779 interdependency in a multimodel ensemble, *J Clim*, 28(13), 5171–5194.
- 780 Schmidt, G., J. Annan, P. Bartlein, B. Cook, É. Guilyardi, J. Hargreaves, S. Harrison,
781 M. Kageyama, A. LeGrande, B. Konecky, et al. (2013), Using palaeo-climate comparisons
782 to constrain future projections in cmip5, *Climate of the Past*, 10(1), 221–250.
- 783 Seneviratne, S. I., M. G. Donat, A. J. Pitman, R. Knutti, and R. L. Wilby (2016), Allowable
784 co 2 emissions based on regional and impact-related climate targets, *Nature*, 529(7587),
785 477.
- 786 Sherwood, S. C., S. Bony, and J.-L. Dufresne (2014), Spread in model climate sensitivity
787 traced to atmospheric convective mixing, *Nature*, 505(7481), 37–42.
- 788 Siler, N., S. Po-Chedley, and C. S. Bretherton (2018), Variability in modeled cloud feed-
789 back tied to differences in the climatological spatial pattern of clouds, *Clim. Dyn.*, 50(3-4),
790 1209–1220.
- 791 Simpson, I. R., and L. M. Polvani (2016), Revisiting the relationship between jet position,
792 forced response, and annular mode variability in the southern midlatitudes, *Geophys Res*
793 *Lett*, 43(6), 2896–2903.
- 794 Stocker, T. F., D. Qin, G.-K. Plattner, M. Tignor, S. K. Allen, J. Boschung, A. Nauels, Y. Xia,
795 V. Bex, P. M. Midgley, et al. (2013), Climate Change 2013. The Physical Science Basis.
796 Working Group I Contribution to the Fifth Assessment Report of the Intergovernmental
797 Panel on Climate Change-Abstract for decision-makers, *Tech. rep.*, Groupe d’experts in-
798 tergouvernemental sur l’evolution du climat/Intergovernmental Panel on Climate Change-
799 IPCC, C/O World Meteorological Organization.
- 800 Su, H., J. H. Jiang, C. Zhai, T. J. Shen, J. D. Neelin, G. L. Stephens, and Y. L. Yung (2014),
801 Weakening and strengthening structures in the hadley circulation change under global
802 warming and implications for cloud response and climate sensitivity, *J. Geophys. Res.*,
803 119(10), 5787–5805.
- 804 Tan, I., T. Storelvmo, and M. D. Zelinka (2016), Observational constraints on mixed-phase
805 clouds imply higher climate sensitivity, *Science*, 352(6282), 224–227.
- 806 Thackeray, C. W., X. Qu, and A. Hall (2018), Why do models produce spread in snow albedo
807 feedback?, *Geophys Res Lett*, 45(12), 6223–6231.
- 808 Tian, B. (2015), Spread of model climate sensitivity linked to double-intertropical conver-
809 gence zone bias, *Geophys Res Lett*.

- 810 Trenberth, K. E., and A. Dai (2007), Effects of mount pinatubo volcanic eruption on the hy-
811 drological cycle as an analog of geoengineering, *Geophys Res Lett*, *34*(15).
- 812 Trenberth, K. E., and J. T. Fasullo (2010), Simulation of present-day and twenty-first-century
813 energy budgets of the southern oceans, *J Clim*, *23*(2), 440–454.
- 814 Volodin, E. (2008), Relation between temperature sensitivity to doubled carbon dioxide and
815 the distribution of clouds in current climate models, *Izvestiya, Atmospheric and Oceanic*
816 *Physics*, *44*(3), 288–299.
- 817 Wagman, B. M., and C. S. Jackson (2018), A test of emergent constraints on cloud feedback
818 and climate sensitivity using a calibrated single-model ensemble, *J Clim*, *31*(18), 7515–
819 7532.
- 820 Wang, J., N. Zeng, Y. Liu, and Q. Bao (2014), To what extent can interannual co2 variabil-
821 ity constrain carbon cycle sensitivity to climate change in cmip5 earth system models?,
822 *Geophys Res Lett*, *41*(10), 3535–3544.
- 823 Wenzel, S., P. M. Cox, V. Eyring, and P. Friedlingstein (2014), Emergent constraints on
824 climate-carbon cycle feedbacks in the cmip5 earth system models, *J. Geophys. Res.*,
825 *119*(5), 794–807.
- 826 Wenzel, S., P. M. Cox, V. Eyring, and P. Friedlingstein (2016), Projected land photosynthesis
827 constrained by changes in the seasonal cycle of atmospheric co₂, *Nature*, *538*(7626), 499.
- 828 Winker, D., J. Pelon, J. Coakley Jr, S. Ackerman, R. Charlson, P. Colarco, P. Flamant, Q. Fu,
829 R. Hoff, C. Kittaka, et al. (2010), The CALIPSO mission: A global 3D view of aerosols
830 and clouds, *Bull. Amer. Meteor. Soc.*, *91*(9), 1211–1229.
- 831 Winkler, A. J., R. B. Myneni, G. A. Alexandrov, and V. Brovkin (2019), Earth system mod-
832 els underestimate carbon fixation by plants in the high latitudes, *Nature communications*,
833 *10*(1), 885.
- 834 Zelinka, M., S. Klein, K. Taylor, T. Andrews, M. Webb, J. Gregory, and P. Forster (2013),
835 Contributions of different cloud types to feedbacks and rapid adjustments in cmip5, *J*
836 *Clim*, *accepted*(2013).
- 837 Zhai, C., J. H. Jiang, and H. Su (2015), Long-term cloud change imprinted in seasonal cloud
838 variation: More evidence of high climate sensitivity, *Geophys Res Lett*, *42*(20), 8729–
839 8737.
- 840 Zhou, C., M. D. Zelinka, A. E. Dessler, and S. A. Klein (2015), The relationship between
841 inter-annual and long-term cloud feedbacks, *Geophys Res Lett*.

⁸⁴² Zhou, C., M. D. Zelinka, and S. A. Klein (2016), Impact of decadal cloud variations on the
⁸⁴³ earth's energy budget, *Nature Geoscience*, 9(12), 871–874.